ACS OMEGA

http://pubs.acs.org/journal/acsodf

Article

Multiparametric Atomic Force Microscopy Identifies Multiple Structural and Physical Heterogeneities on the Surface of *Trypanosoma brucei*

Claire Valotteau,[‖] Andra C. Dumitru,[‖] Laurence Lecordier, David Alsteens, Etienne Pays, David Pérez-Morga,* and Yves F. Dufrêne*

Cite This: *ACS Omega* 2020, 5, 20953−20959

Read Online

ACCESS | Metrics & More | Article Recommendations | Supporting Information

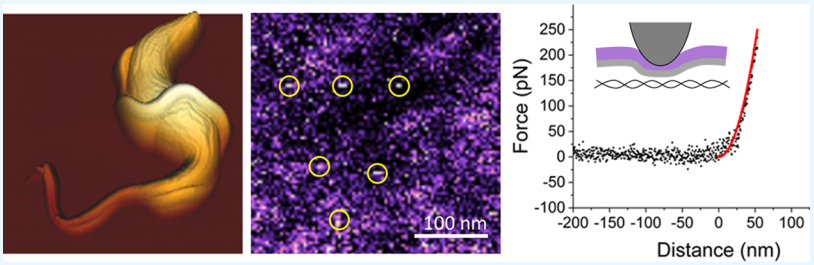

ABSTRACT: A unique feature of the African trypanosome *Trypanosoma brucei* is the presence of an outer layer made of densely packed variable surface glycoproteins (VSGs), which enables the cells to survive in the bloodstream. Although the VSG coat is critical to pathogenesis, how exactly the glycoproteins are organized at the nanoscale is poorly understood. Here, we show that multiparametric atomic force microscopy is a powerful nanoimaging tool for the structural and mechanical characterization of trypanosomes, in a label-free manner and in buffer solution. Directly correlated images of the structure and elasticity of trypanosomes enable us to identify multiple nanoscale mechanical heterogeneities on the cell surface. On a ∼250 nm scale, regions of softer (Young's modulus ∼50 kPa) and stiffer (∼100 kPa) elasticity alternate, revealing variations of the VSG coat and underlying structures. Our nanoimaging experiments show that the *T. brucei* cell surface is more heterogeneous than previously anticipated and offer promising prospects for the design of trypanocidal drugs targeting cell surface components.

INTRODUCTION

The African trypanosome *Trypanosoma brucei* is a parasite responsible for sleeping sickness in humans. Trypanosomes have an elongated cell shape, a highly polarized microtubule cytoskeleton, and a single flagellum attached to the membrane along the cell body.[1] The flagellum is a multifunctional organelle playing roles in cell propulsion, cell morphogenesis, and cytokinesis. The flagellar membrane also favors adhesion to the host and displays virulence factors.[2] A central feature of the *T. brucei* biology is the presence of a dense layer of variant surface glycoproteins (VSGs), which enables the parasite to survive free in the bloodstream of the mammalian host.[1,3−5] VSGs represent the major cell surface proteins (∼95%) and extend ∼15 nm from the cell membrane in the bloodstream form.[4] Throughout the mammalian infectious cycle, the VSG coat fulfills essential functions in pathogenesis, by shielding invariant surface proteins from binding by host antibodies and removing VSG-specific antibodies from the cell surface. This enables the parasite to evade the immune system and establish chronic infection. VSG dimers organize into a very densely packed layer, corresponding to 5×10^6 dimers per cell.[6,7] There is a wide variety of VSGs during infection.[8,9] *T. brucei* uses a repertoire of 2000 VSG genes to switch between different surface variants, a process known as antigenic variation, and it has been estimated that the cell population at any point during infection can express up to 100 VSGs, although dominant VSGs characterize the successive parasitemia waves. The parasite also produces mosaic VSGs, novel variants that form through gene conversion events within VSG sequences. The conformation and diffusion of VSGs have been studied, suggesting that they can adopt two main conformations to respond to obstacles and changes of protein density while maintaining a protective barrier at all times.[7,11]

Another pertinent question is whether the parasite plasma membrane features nanoscale domains, such as lipid rafts. Fluorescence studies have suggested a homogenous structuration of lipids and VSGs on the cell surface.[10,11] By contrast, the

Received: May 22, 2020
Accepted: July 1, 2020
Published: August 13, 2020

https://dx.doi.org/10.1021/acsomega.0c02416
ACS Omega 2020, 5, 20953−20959

formation of small discrete spots of an alanine-rich protein of *T. brucei* has been discussed,[12] suggesting that the proteins are sequestered in lipid rafts. Recently, super-resolution microscopy of bloodstream *T. brucei* cells showed the existence of nanoscale domains within the membrane that were suggested to be associated with the underlying cytoskeleton.[13] In *T. cruzi*, there is evidence that the membrane exhibits discrete 10−150 nm lipid-driven domains bearing different protein compositions.[14,15]

Here, we show that multiparametric atomic force microscopy (AFM) is a powerful nanoimaging platform for the structural and mechanical characterization of the trypanosome cell surface. While AFM has become popular in microbiology for studying bacteria, yeasts, and fungi at the nanoscale,[16−18] only few studies have focused on protozoa.[15] These have been dedicated to the imaging of the flagellum and paraflagellum structures of *T. cruzi*,[19,20] while, to the best of our knowledge, the body of *T. brucei* has never been studied. In this study, we probe the nanostructure and nanomechanics of the *T. brucei* cell surface with the following key questions in mind: how does the cell surface architecture looks like at the nanoscale? How stiff is the cell surface compared to bacterial and mammalian cells? Are the VSG coat and plasma membrane homogenous or do they organize into nanoscale domains? The results show that the parasite surface features multiple nanoscale structural and physical heterogeneities that could be critical for cell surface functions. These experiments suggest that AFM may find broad application in parasitology for studying the complex structure−function relationships of the protozoa cell surface.

RESULTS AND DISCUSSION

Surface Ultrastructure of *Trypanosoma brucei*. We first sought to visualize the morphology and surface architecture of *T. brucei*. Scanning electron microscopy (SEM) revealed the typical elongated, twisted shape of *T. brucei* cells (Figure 1A) but failed to provide high-resolution information on the cell surface. AFM imaging of living trypanosomes proved to be impossible due to the cell motility. Therefore, we optimized a fast, minimally invasive fixation procedure (inspired by ref21, see Methods) that preserves the cell surface while preventing cellular motility. This procedure is known to avoid intramolecular cross-linkers such as glutaraldehyde and paraformaldehyde and is inspired from protocols used for in situ run-on transcription assays. Fluorescence microscopy and electron microscopy analyses showed that this procedure preserves the fast-occurring process of endocytosis, which is evidence for fast-fixation and preservation of cell morphology.[22]

AFM images of whole cells (Figure 1B and Figure S1) confirmed the SEM data and showed the flagellum forming a ridge along the cell body, as well as periodic undulations on the cell surface. Notably, higher resolution images of the cell surface (Figure 1C,D and Figure S1) revealed a wavy morphology, with waves of 81 ± 31 nm in height and 356 ± 87 nm in width (mean ± s.d.; n = 34 from 4 cells), and a surface roughness of 36 ± 15 nm (n = 9 height images of 2 × 2 μm). Wavy patterns were observed with multiple AFM tips and cells, in various orientations, independently from the scanning directions, meaning that they are not due to scanning artifacts (Figure S1). In addition, AFM imaging in multiparametric mapping mode enables a full control of the applied force (see Methods), therefore avoiding any artifact from damaging the cell membrane. The trajectories of these waves roughly follow the long swimming axis of the cell; however, they often cross

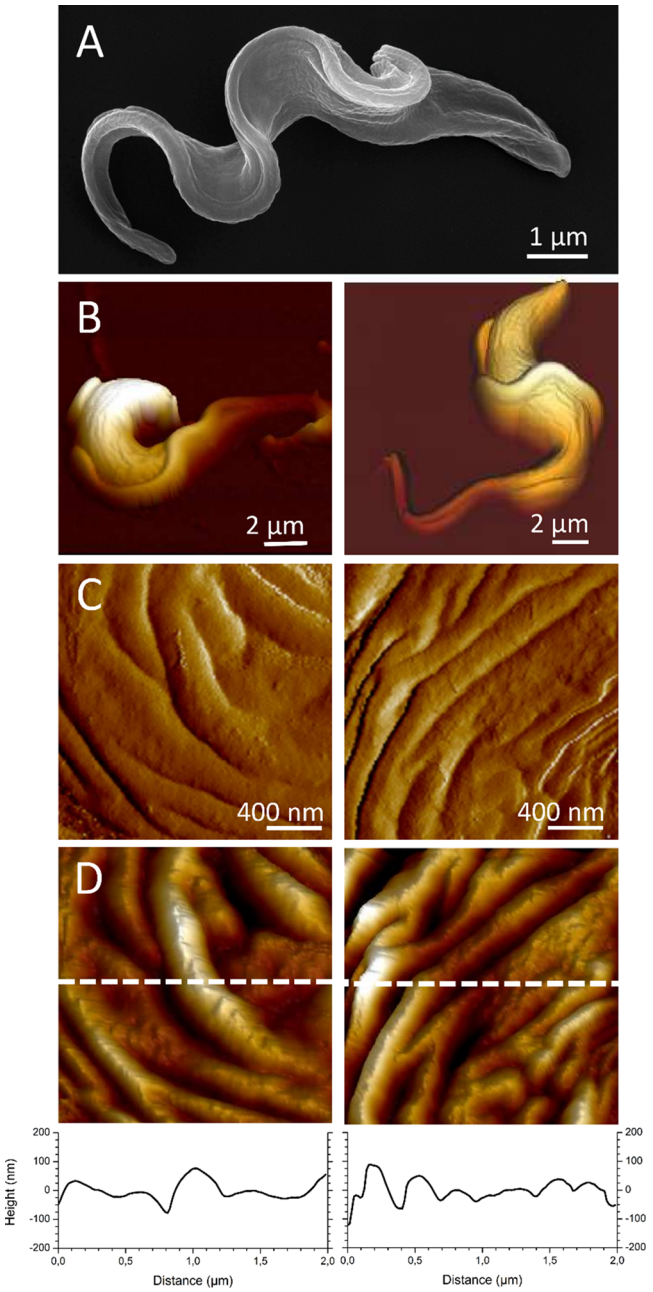

Figure 1. High-resolution imaging of *T. brucei*. (A) SEM image of a strongly fixed *T. brucei* cell. (B) Three-dimensional AFM height images recorded in PBS buffer showing strongly fixed cells immobilized onto glass. (C, D) Error (C) and height (D, color scale: 200 nm) images recorded on two different cells, together with vertical cross-sections taken in the height images along the white lines.

pathways and branch off and into each other. We suggest that these waves might reflect membrane undulations associated with cellular processes. Motility in *T. brucei* is based on a flagellar wave that propagates along the cell.[2] The flagellum follows a helical path around the cell, and lateral attachment of the flagellum to the cell enables the flagellar wave to be directly transmitted to the cell body, causing the entire body to rotate. In response to flagellar beating and confinement, the cell body can deform as defined by changes in the helicity and spacing of the subpellicular microtubule array.[23] Given the heterogeneity of size and trajectory of the observed cell surface waves, we propose that they result from membrane undulations linked to

https://dx.doi.org/10.1021/acsomega.0c02416
ACS Omega 2020, 5, 20953−20959

cellular motility. In *T. brucei*, the inner face of the cytoplasmic membrane is cross-linked to the underlying subpellicular microtubule (SPM) array, consisting of >100 stable microtubules cross-linked with each other.[24] This flexible SPM follows, deforms, and adapts to the movement of the trypanosome propelled by its flagellum.[20] The membrane undulations that we observed could be generated by the bulging of the cell surface that follows and mirrors the deformation of the underlying SMP after the flagellum stroke. During all these rearrangements, the cytoplasmic membrane never detaches from the SPMs due to its cross-linking to the SPMs and to the cohesion of the VSG coat.[21,8,11] Surface undulations could also be associated with cellular structures important for morphogenesis and cell division. Physical and functional connections between the flagellum and cellular structures indeed allow the flagellum to define morphogenetic axes, control organellar inheritance, and orchestrate cell division.[2]

Employing the minimally invasive, non-cross-linking fixation procedure described above, cells could be readily imaged (Figure 2 and Figure S2), featuring a surface roughness of 45 ± 23 nm (n = 8 height images of 2 × 2 μm), thus comparable to that of strongly cross-linked fixed cells. Height images of top of the cells showed a fuzzy contrast (Figure 2 and Figure S2), indicating that the tip interacted with flexible surface molecules, in this case VSGs, the main component. Nevertheless, undulations were observed (Figures 2B and 5A) but less pronounced than those after strong fixation (37 ± 22 nm in height and 414 ± 84 nm in width; mean ± s.d.; n = 20).

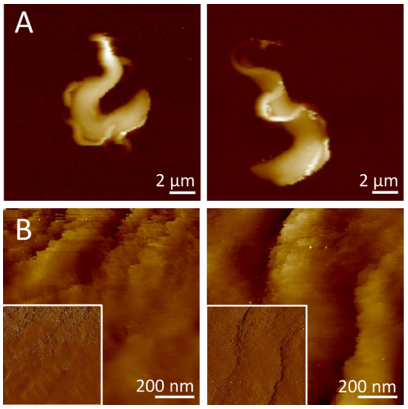

Figure 2. Imaging the *T. brucei* cell surface under minimally invasive conditions. (A) Height images of two different lightly fixed cells recorded in PBS buffer. (B) High-resolution height images (color scale: 200 nm) recorded on two different cells, together with the corresponding error images (insets).

To gain further insights on the VSG organization, lightly fixed cells were mapped with AFM tips functionalized with anti-VSG antibodies (Figure 3). A large proportion of force curves (detection probability of 63%) showed single adhesion events of 62 ± 2 pN magnitude (Gaussian distribution, maximum ± s.d.). This is consistent with the detection of single VSG proteins across the cell surface, as these forces are in the range of those expected for antibody binding at a similar pulling speed (1 μm s^{-1}).[25] The shoulder around 120 pN is likely to be due to the simultaneous detection of two proteins, as expected when proteins are present at high density. These single-molecule data point to the presence of a dense layer of VSG proteins on the cell surface.

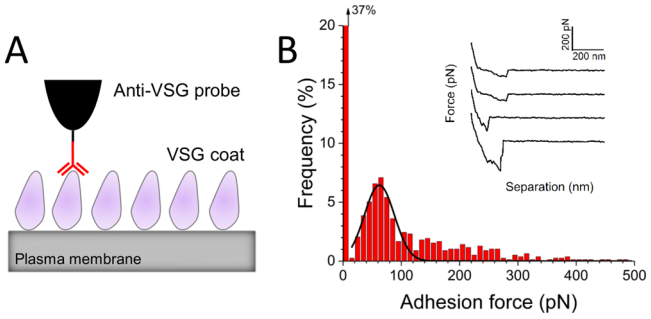

Figure 3. Detecting VSG glycoproteins on the cell surface. (A) To probe single VSG proteins, lightly fixed cells were mapped in the AFM force–volume mode (16 × 16 curves on 2 × 2 μm^2 areas) in PBS buffer using AFM tips terminated with anti-VSG antibodies. (B) Adhesion force histogram (n = 792 force curves from eight different tip-cell combinations) with representative force curves (inset).

Cell Surface Elasticity. Cell mechanics play important roles in cellular functions and disease.[18] With this in mind, we quantified the surface elasticity of *T. brucei* by recording spatially resolved force curves across the cells, converting them into indentation curves, and analyzing them with the Hertz model to assess the Young's modulus (Figure 4A).[26] As shown in Figure 4B, cells featured a wide range of Young's modulus, with values around ∼50, ∼100, and ∼300 kPa being frequently observed (arrows on Figure 4B, illustrated by curves in Figure 4C). This widespread distribution suggests that cells are mechanically heterogeneous, as confirmed below (Figures 5 and 6). Although the origin of cell surface elasticity is unclear, it is likely to be defined by the ∼15 nm thick VSG coat and by the underlying plasma membrane and subpellicular microtubule cytoskeleton. We note that, on average, trypanosomes are stiffer than mammalian cells,[27] consistent with the presence

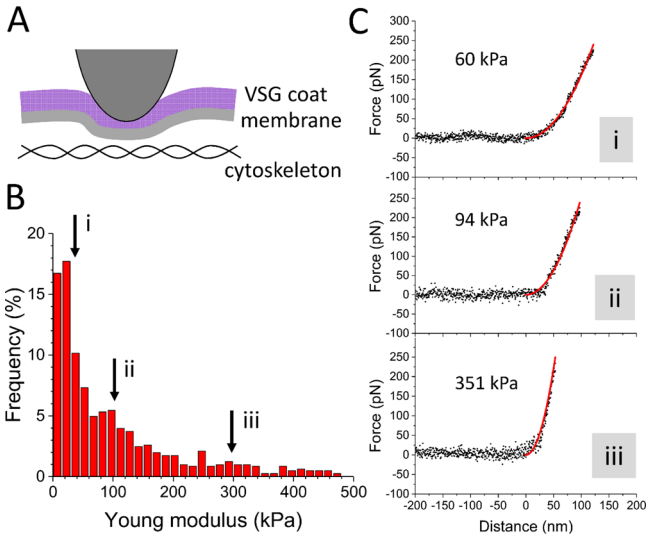

Figure 4. Quantifying cell surface elasticity. (A) Indentation measurements were performed in the AFM force–volume mode to probe cell surface mechanics. (B) Distribution of Young's modulus values assessed by force–volume measurements (16 × 16 curves on 2 × 2 μm^2 areas) on 12 different lightly fixed *T. brucei* cells. (C) Representative force–indentation curves illustrating (i) low, (ii) moderate, and (iii) high cell surface stiffness. The solid lines in red are the theoretical fits (Hertz model) used to extract the Young's modulus.

https://dx.doi.org/10.1021/acsomega.0c02416
ACS Omega 2020, 5, 20953−20959

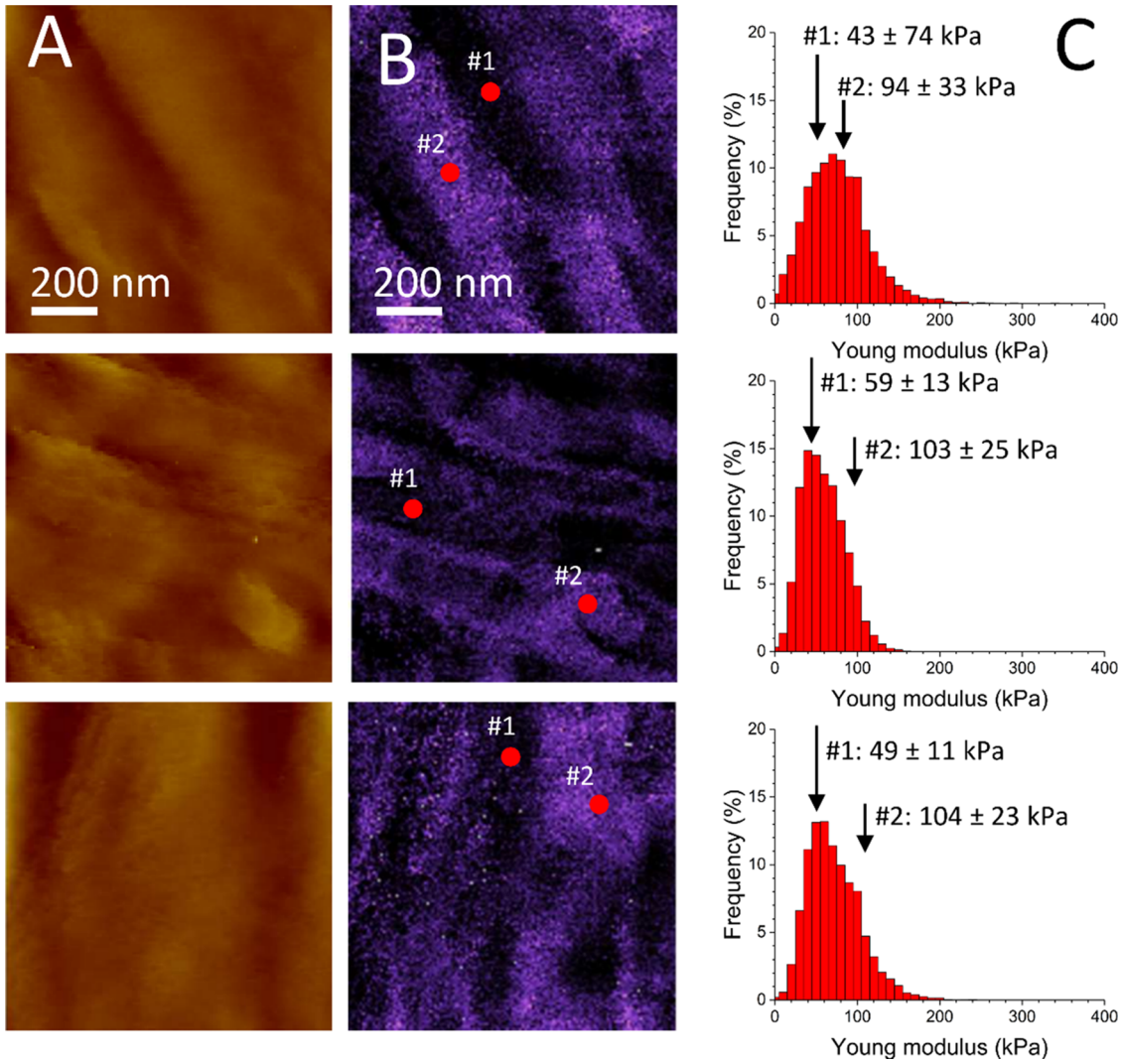

Figure 5. Multiparametric imaging of the cell surface structure and elasticity. (A) AFM FD-based structural images (deconvoluted height signal; color scale: 200 nm) and (B) directly correlated elasticity maps (color scale: 500 kPa) with (C) corresponding Young's modulus histograms obtained on three different lightly fixed cells. Spots #1 and #2 (red dots on B images) illustrate the coexistence of softer and stiffer regions on the same cells (average values in C). Shown here are representative images out of multiple images from 20 cells.

of the densely packed VSG coat, but softer than Gram-positive bacteria and yeasts, known to have a rigid cell wall (~1 MPa).[26,28] The *T. brucei* stiffness is in the range of that of Gram-negative bacteria, whose outer membrane is decorated with a layer of lipopolysaccharides.[29]

The Cell Surface Is Made up of Multiple Structural and Physical Heterogeneities. Plasma membranes are laterally heterogeneous, displaying nanoscale domains such as lipid rafts, which are involved in cellular functions and disease.[30] These assemblies show increased physical stability, as they are more ordered and packed than the surrounding disordered bilayer membrane. A few reports have suggested that membrane heterogeneities occur in parasitic protozoa.[31] For example, the *T. cruzi* surface is highly organized, being structured into nanoscale membrane domains of different compositions.[15] Freeze-fracture electron microscopy images displayed ~30 nm protuberances randomly distributed in both inner and outer plasma membrane leaflets. Biochemical and confocal microscopy studies revealed multiple nanoscale membrane domains bearing different compositions of proteins and lipids.

Whether nanoscale surface domains exist in *T. brucei* is unclear. This prompted us to image the cell surface architecture and elasticity using multiparametric AFM imaging[32,33] (Figures 5 and 6). Force−distance curves were recorded across the cell surface at high frequency, making it possible to image the structure and mechanics at nanometer resolution. AFM images documented multiple nanoscale heterogeneities, which exhibited different elasticities (Figures 5 and 6). On a ~250 nm length scale, regions of softer (dark contrast, ~50 kPa) and stiffer (light contrast, ~100 kPa) elasticity were found to alternate and to correlate with wavy patterns, with the top of the undulations being generally more rigid (Figure 5B,C). There were also localized soft domains surrounded by—alternating with—stiffer material (Figure 6A−D, ellipses and dashed lines).

Interestingly, high-magnification images uncovered a granular organization with a high Young's modulus (typically, 100−500 kPa) (Figure 6A−D), which might reflect the compact assemblies of VSGs. Furthermore, some cells featured on localized areas, very small dots with high stiffness (Figure 6E,F, circles), which might reflect VSG dimers. Indeed, small-angle

https://dx.doi.org/10.1021/acsomega.0c02416
ACS Omega 2020, 5, 20953−20959

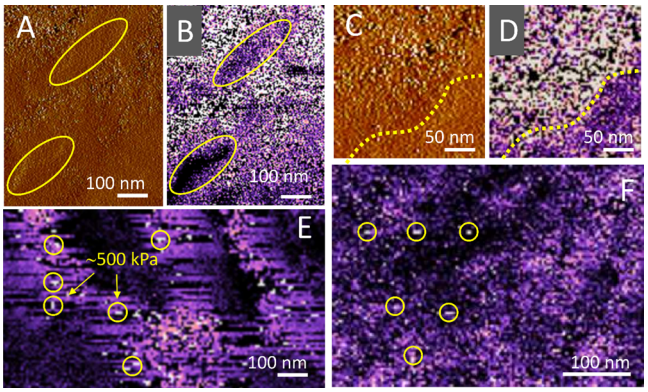

Figure 6. AFM identifies multiple nanoscale heterogeneities on the cell surface. (A, C) FD-based structural images (error signal) and (B, D) directly correlated elasticity maps (color scale: 500 kPa) on gently fixed cells, documenting densely packed granular structures, and ~250−500 nm domains of softer elasticity (ellipses). The dashed lines emphasize the coexistence of soft and stiff areas. (E, F) High-resolution elasticity maps (color scale: 500 kPa) showing highly localized stiff dots (circles). Shown here are representative images out of multiple images from 20 cells.

X-ray scattering experiments have shown that a VSG dimer theoretically occupies ~25 nm^2. Taking into account hydration, rotational freedom and diffusion of the proteins, the total area per dimer was estimated to be ~100 nm^2.[7]

In summary, we identified multiple mechanical heterogeneities on the *T. brucei* cell surface, which may have different origins: (i) variations in the density and conformation of VSGs, (ii) heterogeneous distribution of lipids and non-VSG proteins in the plasma membrane, (iii) organization of underlying cytoskeleton structures, and (iv) indirect influence of flagellum- and cell body-associated structures such as the paraflagellar rod and the flagellum attachment zone.[2] We propose that the heterogeneous distribution of elasticity primarily reflects differences in VSG surface density and conformation. Supporting this view, VSGs have been shown to occupy the cell surface at different densities,[7] by adopting two main conformations while maintaining a protective barrier at all times. This recent study suggested that tightly packed VSGs (i.e., during cell division and/or VSG-switching) can adopt an elongated conformation while still accommodating underlying transmembrane proteins, whereas the relaxed conformation could allow the maintenance of a protective coat on the cell surface even at a reduced protein density. Hence, the coexistence of VSG assemblies with compact and relaxed conformations may explain the occurrence of nanoscale domains with lower and higher mechanical stiffness.

One may argue that gentle fixation may alter the surface properties of the cells. For this reason, we optimized a protocol without cross-linkers. Whenever possible AFM experiments on living cells should be preferred, what can usually be achieved with bacteria and yeasts. However, in the *T. brucei* case, fixation was required and mandatory due to the high mobility of the cells. Without such a light fixation step, no information on cell surface mechanics could have been obtained. Fixation procedures are classically applied to cell membranes for AFM and immunofluorescence analyses, which tend to preserve protein structures. Hinterdorfer et al.[34] could properly image VE-cadherin receptors on animal cells following gentle fixation, a procedure that not only was suitable to prevent the lateral mobility of receptors on the cell surface but also maintains the cell volume and preserves the filamentous structure on the cell cortex. AFM indeed shows that VSG proteins are properly exposed on the entire surface. Regarding the use of fixation for nanomechanical analysis, several studies have indicated that cells exhibit physiologically relevant properties. For instance, Grimm et al.[35] showed by AFM that fixed endothelial cells exhibit physiologically relevant nanomechanics of the cortical actin web. Accordingly, while we cannot exclude that fixation may slightly shift absolute elasticity values, we do believe that our results realistically describe mechanical heterogeneities of the cell surface.

CONCLUSIONS

The VSG coat of *T. brucei* has traditionally been considered as a continuous layer of densely packed VSG dimers, suggesting that the cell surface is structurally and physically homogeneous. We have provided compelling evidence that the parasite surface is highly organized, being structured into specialized nanodomains of lower (10−50 kPa) and higher (up to 500 kPa) mechanical stiffness, which may be important for cellular motility, morphogenesis, division, and adhesion. Our work highlights the potential of AFM to study the structural and physical properties of trypanosomes, which until now had been mostly investigated using fluorescence and electron microscopy techniques. Unique to AFM is the ability to image structural and physical properties with nanoscale resolution, in a label-free manner and directly in buffer solution.

The *T. brucei* surface is decorated with ~100 nm waves, presumably reflecting membrane undulations. Wavy patterns as well as ~250 nm domains are correlated with differences in rigidity, which we believe result from variations in flagellum- and cytoskeleton-associated structures. At higher magnification, the cell surface exhibits a granular morphology with densely packed stiff dots, suggesting variations in VSG density and conformation. Stiff areas of very small size are also present, which are likely to represent individual VSG dimers. We believe that these findings are of biological significance. In living cells, it is now widely accepted that proteins assemble to form surface domains that play functional roles.[36] The mechanical heterogeneities unraveled here may be important for cell surface functions, such as motility, morphogenesis, division, and adhesion. The AFM technology offers promising prospects in antimicrobial therapy, for the design of new trypanocidal drugs targeting cell surface components. The *T. brucei* cell membrane is a target for killing by small hydrophobic peptides that increase the rigidity of lipid bilayers. Similarly, AFM could help testing innovative drugs altering the mechanics, assembly, and function of the VSG coat.

METHODS

Cell Growth and Preparation. Bloodstream-stage *Trypanosoma brucei* parasites were grown in HMI9 supplemented with 10% fetal bovine serum and 10% Serum Plus at 37 °C in 5% CO_2. Cells were fixed either for 30 min at 4 °C (on ice) in 2.5% paraformaldehyde (PFA, strong fixation) or for 5 min at 4 °C (on ice) in 3.5% HCHO (light fixation). Samples were washed 3 times for 5 min and resuspended in 0.1 M sodium cacodylate (Sigma-Aldrich) buffer (pH 7.4). For AFM, cells were then immobilized onto poly-L-lysine-coated glass-bottom Petri dishes (WillCo). Dishes were first filled with a 0.5 mg mL^{-1} poly-L-lysine (PLL, Mw ~70−150 kDa, Sigma) solution in phosphate-buffered saline (PBS, Sigma), incubated at 37 °C

https://dx.doi.org/10.1021/acsomega.0c02416
ACS Omega 2020, 5, 20953−20959

for 30 min, washed with buffer for 3 min, and dried in a laminar flow hood for 2 h at room temperature. The trypanosome suspension was plated onto the PLL-coated dishes for 10 min. Dishes were then washed 3 times with buffer to remove nonattached cells. At least 10 cells per condition were imaged.

AFM Multiparametric Imaging. AFM experiments were performed with a BioScope Resolve AFM (Bruker) operated in the PeakForce QNM mode (NanoScope software v9.2) at ∼25−30 °C in PBS.[37] We used PeakForce QNM Live Cell probes (Bruker) with a tip radius of curvature of 65 nm and spring constants ranging from 0.08 to 0.1 $N{\cdot}m^{-1}$, calibrated by the manufacturer with a vibrometer (OFV-551, Polytec, Waldbronn). The precalibrated spring constant was used to determine the deflection sensitivity using the thermal noise method[38] before each experiment. Unless stated otherwise, the cantilevers were nonfunctionalized. Multiparametric images were acquired using a force setpoint of 100−200 pN. The AFM cantilever was oscillated vertically at 0.25 kHz with peak-to-peak oscillation amplitudes ranging from 100 to 300 nm. Images were recorded using a scan rate of 0.125 Hz and 128 pixels per line. Data were processed offline using the NanoScope Analysis 1.80 Software (Bruker). For mechanical analysis, the retraction part of the curves extracted from PeakForce QNM maps was analyzed to avoid plastic deformation contributions. Best quality fits were obtained when by fitting the contact part of the curve with the Hertz model with a Poisson's ratio of 0.3.[26,28]

Mechanical Measurements by Force−Volume Analysis. Spatially resolved force−distance curves were recorded in the force−volume mode, using a Nanowizard III AFM (JPK Instruments), with OTR4 cantilevers (Olympus, nominal spring constant of 0.02 N m^{-1}). The sensitivity of the cantilever was calibrated by recording a single force curve on a hard surface, and the spring constant was determined using the thermal noise method. Force−distance curves were recorded using a force setpoint of 250 pN, approach and retraction velocities of 1 $\mu m\ s^{-1}$, and a 2 μm ramp size. Measurements were performed by recording 16 × 16 force curves on 2 × 2 μm^2 areas in the center of the cells. Indentations ranged between 50 and 100 nm. Data were analyzed with the data processing software from JPK Instruments (Berlin, Germany). Young's moduli were calculated using the Hertz model (considering a conical tip with an opening angle of 17.5°).

Single-Molecule Detection Using Force−Volume Analysis. AFM tips were functionalized with anti-VSG antibodies previously described.[39] Gold-coated cantilevers (OTR4; Olympus) were immersed overnight in an ethanol solution containing 1 mM 10% 16-mercaptododecahexanoic acid and 90% 1-mercapto-1-undecanol (Sigma), rinsed with ethanol, and dried with N2. Substrates and cantilevers were then immersed for 30 min in a solution containing 10 $mg\ ml^{-1}$ NHS and 25 $mg.ml^{-1}$ 1-ethyl-3-(3dimethylaminopropyl)-carbodiimide (Sigma), rinsed with ultrapure water (ELGA LabWater), incubated with 0.1 $mg\ ml^{-1}$ anti-VSG antibodies for 1 h, rinsed further with PBS buffer, and then immediately used without drying. Single-molecule force spectroscopy was performed using a Nanowizard III AFM (JPK Instruments). The cantilever spring constants were measured by the thermal noise method. Adhesion force maps were obtained by recording 16 × 16 curves on 2 × 2 μm^2 areas on the top of the cells. All curves were recorded using a maximum applied force of 250 pN, a contact time of 100 ms, and constant approach and retraction speeds of 1 $\mu m\ s^{-1}$. Data were analyzed with the data processing software from JPK Instruments (Berlin, Germany).

SEM Imaging. Samples were fixed overnight at 4 °C in glutaraldehyde 2.5% and 0.1 M cacodylate buffer (pH 7.2) and post-fixed in OsO4 (2%) in the same buffer. After serial dehydration, samples were dried at the critical point and coated with platinum by standard procedures. Observations were made using a Tecnai FEG ESEM QUANTA 200 (FEI) and images processed by the SIS iTEM (Olympus) software.

■ ASSOCIATED CONTENT

Supporting Information

The Supporting Information is available free of charge at https://pubs.acs.org/doi/10.1021/acsomega.0c02416.

(Figure S1) Imaging chemically fixed *T. brucei* cells; (Figure S2) imaging the *T. brucei* cell surface under minimally invasive conditions (PDF)

■ AUTHOR INFORMATION

Corresponding Authors

David Pérez-Morga − *Laboratory of Molecular Parasitology, IBMM, Université Libre de Bruxelles, B-6041 Gosselies, Belgium*; Email: David.Perez-Morga@ulb.ac.be

Yves F. Dufrêne − *Louvain Institute of Biomolecular Science and Technology, UCLouvain, B-1348 Louvain-la-Neuve, Belgium; Walloon Excellence in Life sciences and Biotechnology (WELBIO), B-1300 Wavre, Belgium;* orcid.org/0000-0002-7289-4248; Email: yves.dufrene@uclouvain.be

Authors

Claire Valotteau − *Louvain Institute of Biomolecular Science and Technology, UCLouvain, B-1348 Louvain-la-Neuve, Belgium*

Andra C. Dumitru − *Louvain Institute of Biomolecular Science and Technology, UCLouvain, B-1348 Louvain-la-Neuve, Belgium*

Laurence Lecordier − *Laboratory of Molecular Parasitology, IBMM, Université Libre de Bruxelles, B-6041 Gosselies, Belgium*

David Alsteens − *Louvain Institute of Biomolecular Science and Technology, UCLouvain, B-1348 Louvain-la-Neuve, Belgium;* orcid.org/0000-0001-9229-113X

Etienne Pays − *Laboratory of Molecular Parasitology, IBMM, Université Libre de Bruxelles, B-6041 Gosselies, Belgium*

Complete contact information is available at: https://pubs.acs.org/10.1021/acsomega.0c02416

Author Contributions

‖C.V. and A.C.D. contributed equally. C.V., A.C.D., L.L., D.A., E.P., D.P.M., and Y.F.D. designed the experiments, analyzed the data, and wrote the article. C.V. and A.C.D. collected the data.

Notes

The authors declare no competing financial interest.

■ ACKNOWLEDGMENTS

Work at the Université catholique de Louvain was supported by the European Research Council (ERC) under the European Union's Horizon 2020 research and innovation program (grant agreement No [693630]), the National Fund for Scientific Research (FNRS), the FNRS-WELBIO (Grant n°WELBIO-CR-2015A-05), and the Research Department of the

Communauté française de Belgique (Concerted Research Action). Y.F.D. is a Research Director at the FNRS. Work at the ULB was funded by the ERC (grant 669007-APOLs), FNRS (grant J.0091.17), and the Communauté française de Belgique (ARC Advanced). We thank S.U. and D.M. for help with confocal microscopy and SEM, respectively.

REFERENCES

(1) Matthews, K. R. The developmental cell biology of *Trypanosoma brucei*. *J. Cell Sci.* **2005**, *118*, 283−290.
(2) Langousis, G.; Hill, K. L. Motility and more: the flagellum of *Trypanosoma brucei*. *Nat. Rev. Microbio.* **2014**, *12*, 505−518.
(3) Schwede, A.; Macleod, O. J.; MacGregor, P.; Carrington, M. How does the VSG coat of bloodstream form African trypanosomes interact with external proteins? *PLoS Pathog.* **2015**, *11*, No. e1005259.
(4) Mugnier, M. R.; Stebbins, C. E.; Papavasiliou, F. N. Masters of disguise: antigenic variation and the VSG coat in *Trypanosoma brucei*. *PLoS Pathog.* **2016**, *12*, No. e1005784.
(5) Bangs, J. D. Evolution of Antigenic Variation in African Trypanosomes: Variant Surface Glycoprotein Expression, Structure, and Function. *BioEssays* **2018**, *40*, 1800181.
(6) Jackson, D. G.; Owen, M. J.; Voorheis, H. P. A new method for the rapid purification of both the membrane-bound and released forms of the variant surface glycoprotein from *Trypanosoma brucei*. *Biochem. J.* **1985**, *230*, 195−202.
(7) Bartossek, T.; Jones, N. G.; Schäfer, C.; Cvitković, M.; Glogger, M.; Mott, H. R.; Kuper, J.; Brennich, M.; Carrington, M.; Smith, A. S.; Fenz, S.; Kisker, C.; Engstler, M. Structural basis for the shielding function of the dynamic trypanosome variant surface glycoprotein coat. *Nat. Microbiol.* **2017**, *2*, 1523−1532.
(8) Hall, J. P.; Wang, H.; Barry, J. D. Mosaic VSGs and the scale of *Trypanosoma brucei* antigenic variation. *PLoS Pathog.* **2013**, *9*, No. e1003502.
(9) Mugnier, M. R.; Cross, G. A.; Papavasiliou, F. N. The *in vivo* dynamics of antigenic variation in *Trypanosoma brucei*. *Science* **2015**, *347*, 1470−1473.
(10) Buelow, R.; Overath, P.; Davoust, J. Rapid lateral diffusion of the variant surface glycoprotein in the coat of *Trypanosoma brucei*. *Biochemistry* **1988**, *27*, 2384−2388.
(11) Hartel, A. J.; Gloggler, M.; Jones, N. G.; Abuillan, W.; Batram, C.; Hermann, A.; Fenz, S.; Tanaka, M.; Engstler, M. N-glycosylation enables high lateral mobility of GPI-anchored proteins at a molecular crowding threshold. *Nat. Commun.* **2016**, *7*, 12870.
(12) Nolan, D. P.; Jackson, D. G.; Biggs, M. J.; Brabazon, E. D.; Pays, A.; Van Laethem, F.; Paturiaux-Hanocq, F.; Elliot, J. F.; Voorheis, H. P.; Pays, E. Characterization of a novel alanine-rich protein located in surface microdomains in *Trypanosoma brucei*. *J. Biol. Chem.* **2000**, *275*, 4072−4080.
(13) Glogger, M.; Subota, I.; Pezzarossa, A.; Denecke, A. L.; Carrington, M.; Fenz, S.; Engstlera, M. Facilitating trypanosome imaging. *Exp. Parasitol.* **2017**, *180*, 13−18.
(14) de Souza, W.; Rocha, G. M. Atomic force microscopy: a tool to analyze the structural organization of pathogenic protozoa. *Trends Parasitol.* **2011**, *27*, 160−167.
(15) Mucci, J.; Lantos, A. B.; Buscaglia, C. A.; Leguizamón, M. S.; Campetella, O. The *Trypanosoma cruzi* Surface, a Nanoscale Patchwork Quilt. *Trends Parasitol.* **2017**, *33*, 102−112.
(16) Xiao, J.; Dufrêne, Y. F. Optical and force nanoscopy in microbiology. *Nat. Microbiol.* **2016**, *1*, 16186.
(17) Dufrêne, Y. F.; Ando, T.; Garcia, R.; Alsteens, D.; Martinez-Martin, D.; Engel, A.; Gerber, C.; Müller, D. J. Imaging modes of atomic force microscopy for application in molecular and cell biology. *Nat. Nanotechnol.* **2017**, *12*, 295.
(18) Krieg, M.; Fläschner, G.; Alsteens, D.; Gaub, B. M.; Roos, W. H.; Wuite, G. J. L.; Gaub, H. E.; Gerber, C.; Dufrêne, Y. F.; Müller, D. J. Atomic force microscopy-based mechanobiology. *Nat. Rev. Phys.* **2019**, *1*, 41−57.
(19) Rocha, G. M.; Teixeira, D. E.; Miranda, K.; Weissmüller, G.; Mascarello Bisch, P.; de Souza, W. Structural changes of the paraflagellar rod during flagellar beating in *Trypanosoma cruzi*. *PLoS One* **2010**, *5*, No. e11407.
(20) Hughes, L. C.; Ralston, K. S.; Hill, K. L.; Zhou, Z. H. Three-dimensional structure of the Trypanosome flagellum suggests that the paraflagellar rod functions as a biomechanical spring. *PLoS One* **2012**, *7*, No. e25700.
(21) Navarro, M.; Gull, K. A pol I transcriptional body associated with VSG mono-allelic expression in *Trypanosoma brucei*. *Nature* **2001**, *414*, 759.
(22) Vanwalleghem, G.; Fontaine, F.; Lecordier, L.; Tebabi, P.; Klewe, K.; Nolan, D. P.; Yamaryo-Botté, Y.; Botté, C.; Kremer, A.; Schumann Burkard, G.; Rassow, J.; Roditi, I.; Pérez-Morga, D.; Pays, E. Coupling of lysosomal and mitochondrial membrane permeabilization in trypanolysis by APOL1. *Nat. Commun.* **2015**, *6*, 8078.
(23) Sun, S. Y.; Kaelber, P. T.; Chen, M.; Dong, X.; Nematbakhsh, Y.; Shi, J.; Dougherty, M.; Lim, C. T.; Schmid, M. F.; Chiu, W.; He, C. Y. Flagellum couples cell shape to motility in *Trypanosoma brucei*. *Proc. Natl. Acad. Sci. U. S. A.* **2018**, *115*, e5916−e5925.
(24) Sherwin, T.; Gull, K. The cell division cycle of Trypanosoma brucei brucei: timing of event markers and cytoskeletal modulations. *Philos. Trans. R. Soc. B.* **1989**, *323*, 573−588.
(25) Müller, D. J.; Helenius, J.; Alsteens, D.; Dufrene, Y. F. Force probing surfaces of living cells to molecular resolution. *Nat. Chem. Biol.* **2019**, *5*, 383−390.
(26) Touhami, A.; Nysten, B.; Dufrêne, Y. F. Nanoscale mapping of the elasticity of microbial cells by atomic force microscopy. *Langmuir* **2003**, *19*, 4539−4543.
(27) Matzke, R.; Jacobson, K.; Radmacher, M. Direct, high-resolution measurement of furrow stiffening during division of adherent cells. *Nat. Cell Biol.* **2001**, *3*, 607.
(28) Francius, G.; Domenech, O.; Mingeot-Leclercq, M. P.; Dufrêne, Y. F. Direct observation of *Staphylococcus aureus* cell wall digestion by lysostaphin. *J. Bacteriol.* **2008**, *190*, 7904−7909.
(29) Gaboriaud, F.; Bailet, S.; Dague, E.; Jorand, F. Surface structure and nanomechanical properties of *Shewanella putrefaciens* bacteria at two pH values (4 and 10) determined by atomic force microscopy. *J. Bacteriol.* **2005**, *187*, 3864−3868.
(30) Sezgin, E.; Levental, I.; Mayor, S.; Eggeling, C. The mystery of membrane organization: composition, regulation and roles of lipid rafts. *Nat. Rev. Mol. Cell. Biol.* **2017**, *18*, 361.
(31) de Souza, W. Macro, micro and nano domains in the membrane of parasitic protozoa. *Parasitol. Int.* **2007**, *56*, 161−170.
(32) Alsteens, D.; Trabelsi, H.; Soumillion, P.; Dufrêne, Y. F. Multiparametric atomic force microscopy imaging of single bacteriophages extruding from living bacteria. *Nat. Commun.* **2013**, *4*, 2926.
(33) Dufrêne, Y. F.; Martínez-Martín, D.; Medalsy, I.; Alsteens, D.; Müller, D. J. Multiparametric imaging of biological systems by force-distance curve−based AFM. *Nat. Methods* **2013**, *10*, 847−854.
(34) Chtcheglova, L. A.; Waschke, J.; Wildling, L.; Drenckhahn, D.; Hinterdorfer, P. Nano-scale dynamic recognition imaging on vascular endothelial cells. *Biophys. J.* **2007**, *93*, L11−L13.
(35) Grimm, K. B.; Oberleithner, H.; Fels, J. Fixed endothelial cells exhibit physiologically relevant nanomechanics of the cortical actin web. *Nanotechnology* **2014**, *25*, 215101.
(36) Ikonen, E. Roles of lipid rafts in membrane transport. *Curr. Opin. Cell Biol.* **2001**, *13*, 470−477.
(37) Dumitru, A. C.; Poncin, M. A.; Conrard, L.; Dufrêne, Y. F.; Tytecab, D.; Alsteens, D. Nanoscale membrane architecture of healthy and pathological red blood cells. *Nanoscale Horiz.* **2018**, *3*, 293−304.
(38) Hutter, J. L.; Bechhoefer, J. Calibration of atomic-force microscope tips. *Rev. Sci. Instrum.* **1993**, *64*, 1868−1873.
(39) O'Beirne, C.; Lowry, C. M.; Voorheis, H. P. Both IgM and IgG anti-VSG antibodies initiate a cycle of aggregation-disaggregation of bloodstream forms of *Trypanosoma brucei* without damage to the parasite. *Mol. Biochem. Parasitol.* **1998**, *91*, 165−193.

https://dx.doi.org/10.1021/acsomega.0c02416
ACS Omega 2020, 5, 20953−20959